An Investigation into the Liquid Sloshing Characteristics of Ground Anchored Tanks during Lateral Vibration

R. Sreekala*, A. Meher Prasad[1] and K. Muthumani*
*Scientist, CSIR-SERC, CSIR-Structural Engineering Research Centre, Chennai, India
[1]Professor, Indian Institute of Technology, Madras, Chennai, India
E-mail: kala@serc.res.in/kalachn@gmail.com

ABSTRACT

Sloshing is one of the major concerns for liquid storage tanks and the vibration characteristics of the contained liquid require lot of research attention. Simulated experimental investigations using triaxial shake tables are rare in this field and the non linear dynamic behavior of the structure is of interest, be it during transportation of liquids or during earthquakes. The paper presents an experimental cum analytical investigation on lateral sloshing behavior under simulated vibrating conditions on a fixed base rectangular container with water. The tank has been designed to suit experimental requirements and the walls were made of Perspex sheets in order to view the sloshing phenomena and for image capturing purposes. The behavior of the system is identified during dynamic loading under lateral sweep sine excitation and simulated random vibration studies were carried out further on the 3D shaking table. Sloshing natural frequencies, wave amplitudes and dynamic pressures on the tank walls are measured during the investigation which throws light into the nonlinear dynamic characteristics due to large amplitude sloshing. CFD modeling has been carried out on the experiments conducted and the results are discussed.

Key words: Dynamic behaviour of liquid tanks, Sloshing, Wave Amplitude, Hydro dynamic Pressures, Computational modelling

1. INTRODUCTION AND SIGNIFICANCE OF THE STUDY

Vibration characteristics of liquid containers are of research interest for the past few decades and the development of nonlinearities during random vibration, control many of its applications. Sloshing is characterized by the oscillation of unrestrained free surface of the liquid in a partially filled container due to external excitation. The special NASA monograph edited by Abramson (Abramson, 1966) addressed the sloshing problems encountered in aerospace vehicles. Sloshing will be of concern not only in onshore tanks, road vehicles, but in offshore structures like platforms, jacket, mono towers, etc. Sloshing has been observed in the ballast tanks of a tension leg platform. It can also occur in an oil gas separator on a floating off shore platform. Oil gas separators are used to separate the oil, gas and water during oil production. Sloshing can be excited by wave induced motions of the platform. The consequence of sloshing is a mixing effect on the oil, water and gas that delays oil production. Extensive numerical and few experimental investigations were carried out on this topic by researchers in the past few decades (Kana, 1966, Faltinsen et al, 2000, Faltinsen & Timokha, 2002, Ibrahim, 2005).

Experimental studies on liquid surface oscillations in longitudinally excited compartmented cylindrical and spherical tanks were carried out by KANA,1966. The liquid free surface during sloshing can experience various types of motion like simple planar, non-planar, rotational, irregular beating, symmetric, asymmetric, quasi periodic and chaotic(Ibrahim, 2005). Whatever be the excitation, normally amplitude of slosh is found to depend upon the amplitude and frequency of tank motion, fill depth and properties of liquid and the tank geometry. When the external forcing frequency gets nearer to the natural frequency of the liquid, resonance and hence severe sloshing occurs.

The influence of liquid viscosity on the sloshing modes natural frequencies was studied analytically and experimentally for rectangular tanks by Scarsi (1971). Scarsi found that the fluid viscosity affects the values of the natural frequencies only for low values of fluid depth ratio. Su (1981) considered the effect of fluid viscosity on the vibration of elastic shells by studying the axisymmetric free-surface

oscillations of a fluid-filled spherical shell. Henderson and Miles (1994) calculated the natural frequencies and damping ratios for surface waves in a circular cylinder based on the assumption of a fixed contact line, Stokes boundary layers, and either a clean or a fully contaminated surface. Two fluid flow instability problems that are difficult to solve is handled using explicit schemes (Sen Gupta et al, 2004). Solution of Navier Stokes equation by various formulations have been found to be robust in nonlinear flow (Sengupta et al, 2010). The inherent liquid viscosity in tanks without baffles is found to have a very limited effect in reducing the sloshing amplitude (Ibrahim, 2005). Here in the present study, the objective is to investigate the behavior during large amplitude sloshing, viscosity effects are not considered. Regarding the lateral force developed on tank walls, the liquid used for the study namely water gives conservative estimates.

Many researchers have devoted their efforts to study sloshing analytically based on potential flow theory. Faltinsen derived a linear analytical solution for liquid sloshing in a horizontally excited 2-D rectangular tank and this solution has been widely used in the validation of numerical models. Moiseev (1958) carried out a pioneering analytical study on nonlinear resonant sloshing. Moiseev's detuning Duffing like asymptotic have been derived. Later Faltinsen and Timokha (2002) developed a multimodal approach to describe the nonlinear sloshing in a rectangular tank with finite water depth. Hill, 2003 analyzed the transient behavior of the resonated waves by relaxing many of the assumptions adopted in the previous studies. However, these theoretical analyses are not valid for viscous and turbulent flows, so the overturning and breaking waves during violent liquid sloshing could not be described. Many of the numerical developments using Finite Element Method (FEM), Finite Difference Method (FDM) and Boundary Element Method (BEM) which are grid based are two dimensional in nature and are not compared with the actual experimental data. Kim (2001) and Kim et al. (1994) employed the SOLA scheme to study liquid sloshing in a 3-D container and adopted the concept of buffer zone to calculate the impact pressure on the tank ceiling and is not valid for broken free surface. A new high spectral accuracy compact difference scheme is proposed for problems with non-periodic boundary condition (Sengupta, 2004). Liquid sloshing in an oscillating tank is simulated numerically using moving grid and body force method adopting Arbitrary Langrangean Eulerian (ALE) level set method (Watanabe, 2011). Smoothed Particle Hydrodynamics (SPH) with an improved approximation scheme with corrections on kernel gradient and density is being tried for large amplitude sloshing and free surface fragmentation (Rafiee et al., 2011).

A 3D model that can simulate viscous liquid sloshing with broken free surfaces are ongoing all around the world. Liquid storage tanks belong to those classes of structures in which their value to society far exceeds the economic worth of both the tanks and their contents. Normally effects of sloshing are not considered in the design of liquid storage tanks. Nonlinear effects are always present in reality during lateral sloshing and they sometimes dominate the sloshing response. During past earthquakes, liquid storage tanks have suffered varying degree of damages. The hazardous effect of liquid sloshing and the extensive damage sustained by liquid-filled tanks were evident in past seismic events such as the 1964 Alaska, the 1964 Niigata, the 1968 Tokachi-Oki, the 1979 Imperial Valley, the 1983 Coalinga, and more recently, the 1989 Loma Prieta, the 1992 Landers and the 1994 Northridge earthquakes. Documented case histories of actual storage tanks in strong earthquakes are limited. But there are numerous reports on loss of contents of the tank, fires, and rupture of pipeline attachments to tank walls rather than the failure of the tank walls itself. A foremost task in evaluating the seismic safety of a liquid container is to evaluate the hydrodynamic forces of the sloshing liquid exerted on the structure. The wave amplitude and hydrodynamic pressure distribution on tank walls are of important criteria to be examined during random excitation of liquid tanks. As far as the documented evidence of tank damages, Manos and Clough, 1985 describes the tank damages due to 1983 Coalinga earthquake. Hatayama (2008) described severe earthquake-induced sloshing damage to seven large oil storage tanks with floating roof structures as the consequence of the 2003 Tokachi-oki earthquake in northern Japan, which generated large amplitude long-period (4–8 sec) ground motions. In order to identify the damage potential of ground motion time histories, there are methods based on wavelet analysis and methods based on entropy principle to identify resonant accelerograms. Some recent tools to investigate the well known pulse like ground motion records and recent earthquakes have been applied by researchers (Sreekala et al., 2011).

Non linear slosh effects can be due to complex geometries, large wave amplitudes or due to the instabilities and hence involve different forms of sloshing (Abramson et. al., 1974). When the wave amplitude is large enough to cause nonlinear effects, the linearized theory is not valid. Neglecting viscous effects, the nonlinear slosh theory can be derived from velocity potential and the liquid velocities are still

given by spatial derivatives of the potential. The use of the linear wave theory has restricted in many ways the true behaviour of liquid sloshing which may lead to underestimation of the structural response of the container. Underestimation of the sloshing height leads to an unsafe freeboard design in the container which caused numerous damages in the roof-wall connection during past earthquakes. A linear sloshing model proposed by Housner, 1963 has been widely used and adopted in many of the current ground-based tank standards such as the API 650 and the AWWA D10013 because of its simplicity. On the other hand, the non-linear wave approach has not been attempted in predicting the vibration response of tank structures because of its mathematical difficulties in determining the elevation of the unknown moving free-surface and in evaluating the geometrically non-linear boundary conditions on the liquid surface.

The study confirms the fact that in a resonant phenomenon like sloshing, the maximum amplitude of input excitations are capable of creating dynamic nonlinear wave regimes in fluid flow during random vibrations like earthquakes. Even though linear theories are most widely used to represent the parameters of interest like highest sloshing period, wave height and dynamic pressures, the nonlinearities emerging out of tank liquid motions are significant for the local stresses. Swirling or rotary wave motions can also occur during harmonic horizontal excitation of liquid in the nearly square base tanks when the forcing frequency is in the vicinity of the lowest natural frequency. The nature of turbulence during external excitation in a partially filled tank is primarily due to sloshing and pressure gradient. Liquid pressure impacts are a source of strong non linearity in a liquid tank system. The experiences during earthquakes are proofs for the same and hence the nonlinearities emerging out of the phenomena should be properly accounted in the design of such structures.

2. EXPERIMENT SET UP AND MEASUREMENTS TAKEN

In order to investigate the sloshing behaviour, experiments were conducted in a tri axial shaking table of 5 ton capacity in ASTaR Lab, CSIR -SERC. A simple experimental set up was designed and fabricated to conduct experiments for measuring the dynamic parameters during excitation. The tank has been designed to suit the experimental objectives and the dimensions were selected to fit the structure in the 2 m- Shaking Table. The plan dimension of the tank is 1.2 m ∞ 1.0 m with a height of 1.0 m. The base of the tank and the frame was fabricated in steel and a possible arrangement is made to fix the structure on the shaking table. The walls were made of Perspex sheets (Acrylic based-12 mm thick) in order to view the sloshing phenomena experimentally and for image capturing purposes.

A sloshing probe has been developed to record the free surface wave height which consists of non contact displacement sensors. Two non contact sensors were used to collect the wave height information which captures the data along the mid and corner width of the tank respectively. The whole arrangement consisting of wave height and acceleration measurement on two locations, was fabricated in a wooden frame which is movable to different locations of interest. The photograph of the test set up is shown in Fig. 2.1(a). The device developed recorded the free surface wave heights and simultaneously acceleration
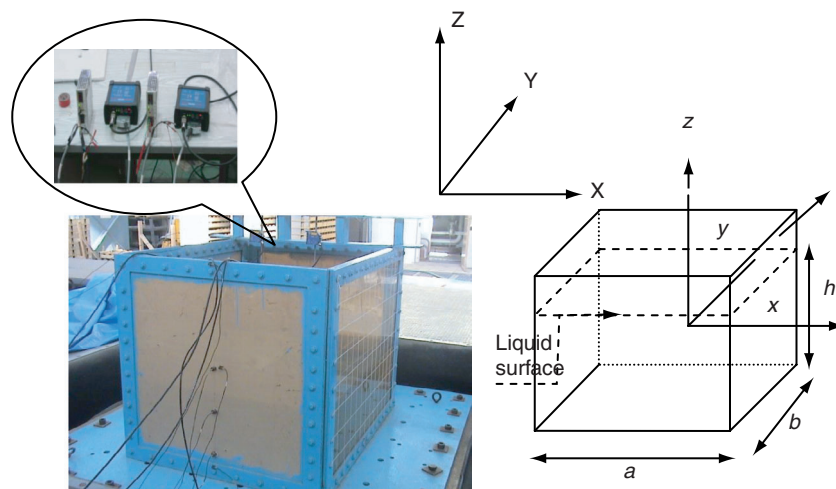

Figure 2.1. (a) The Experimental set up with various sensors – The non contact slosh height instrumentation in the inset (b) Co-ordinate system used for the tank.

of the liquid inside the tank was also recorded. The test data were collected at twelve other locations along the length of the tank during sweep sine and earthquake excitations. Pressure sensors were calibrated and installed at three locations along the height of the tank. Pressure gauges were installed at 0.12 m, 0.33 m, and 0.53 m from the tank bottom respectively. The sensors were used in conjunction with a signal processing unit where it collects the data in terms of voltage signal between 0 V and 10 V. The electrical signals are continuously recorded with the help of 16-channel data acquisition system.

The liquid filled tank up to a height of 0.64 m is mounted on the tri axial shake table and sweep sine and further harmonic tests were carried out. Shaking table tests are known for its excellent control features be it on amplitude or acceleration and it was adequately provided during sweep sine tests. The behavior of the system is identified during dynamic loading using sinusoidal harmonic excitation at the sloshing frequency, after conducting a sweep sine test in the frequency range 0.25–5 Hz, in the lateral direction. Experiments conducted on the tri-axial shaking table system helped to further investigate on the quantities of interest such as hydro dynamic pressure on the wall, accelerations inside the liquid and outside tank wall, sloshing height of the liquid. The natural frequencies of sloshing, obtained experimentally during sweep tests were compared with the available theoretical results and the following section describe this. Fig. 2.1(b). shows the Cartesion x, y, z co-ordinate system used for the derivation of the slosh equation. The x, y, z co-ordinate system is fixed to and moves with the tank, whereas the inertial X, Y, Z co-ordinate system is stationary.

2.1. Natural modes

For the derivation of sloshing natural modes, the liquid considered is inviscid and the motion is assumed without vorticity. The slosh velocity distribution can be derived from a velocity potential Φ. The x, y, z components of the velocity u, v, w are computed from the spatial derivative of the potential,

$$u = \frac{\partial \Phi}{\partial x} \quad v = \frac{\partial \Phi}{\partial y} \quad w = \frac{\partial \Phi}{\partial z}$$

The condition of liquid incompressibility which the velocity potential Φ need to satisfy everywhere in the liquid volume is given by the following differential equation,

$$\nabla^2 \Phi = 0 \tag{2.1.1}$$

For a potential flow that does not contain vorticity, the fluid dynamics equation of motion can be integrated directly to give the unsteady form of Bernaulli equation:

$$\frac{\partial \Phi}{\partial t} + \frac{p}{\rho} + gz + \frac{1}{2}\left(u^2 + v^2 + w^2\right) = f(t) \tag{2.1.2}$$

here 'p' is the fluid pressure, 'ρ' is the fluid density, and g is the effective gravity. Neglecting the higher powers, and absorbing the constant of integration $f(t)$ in the definition of Φ, the linearized form of the above equation is thus,

$$\frac{\partial \Phi}{\partial t} + \frac{p}{\rho} + gz = 0 \tag{2.1.3}$$

The complete solution of the Eqn. 2.1.1 should satisfy the boundary conditions at the free surface and at the tank walls, and the Eigen functions can be obtained for various motions of the tank. The boundary conditions which need to be satisfied are stated as follows.
1) At the wetted rigid wall and bottom, the velocity component normal to the boundary must vanish.
2) At the free surface, the pressure is zero, which is obtained from the Eqn. 2.1.3, after setting $p = 0$ for $z = h/2$.
3) The vertical velocity of a fluid particle located on the free surface should equal to the vertical velocity of the free surface itself. This condition is known as the kinematic condition. Assuming, $\delta(x, y, t)$ is the small displacement of the free surface, above the undisturbed level, $z = h/2$.

A kinematic condition is needed to relate the surface displacement δ to the vertical component of the liquid velocity at the surface and this condition in the linearized form is simply,

$$\frac{\partial \delta}{\partial t} = w = \frac{\partial \Phi}{\partial z} \quad \text{for} \quad z = h/2, \tag{2.1.4}$$

Differentiating Eqn. 2.1.3 with respect to t and differentiating Eqn. 2.1.4 with respect to z, and combining the two equations to eliminate δ,

$$\frac{\partial^2 \Phi}{\partial t^2} + g \frac{\partial \Phi}{\partial z} = 0 \quad \text{for} \quad z = h/2 \tag{2.1.5}$$

This Eqn. 2.1.5 consisting of the time derivative of ϕ involve the natural frequencies of sloshing and the equation shows that these frequencies are directly related to the imposed gravitational field. The roots of these eigen functions represent the natural frequencies of the sloshing liquid (Graham et. al, 1952). The solution ω_n for the natural frequency can be expressed as

$$\omega_n^2 = \pi(2n-1)\left(\frac{g}{a}\right) \tanh\left[\pi(2n-1)\left(\frac{h}{a}\right)\right] \tag{2.1.6}$$

where the subscript n indicates the mode number for a rectangular tank of width a containing liquid of height h. The anti symmetric modes are capable of producing lateral forces or torques and the slosh wave shape can be expressed in the cartesian coordinate system as

$$-\frac{A}{a\omega_n}(2n-1)\sinh\left[\pi(2n-1)\left(\frac{h}{a}\right)\right]\sin\left[\pi(2n-1)\left(\frac{x}{a}\right)\right]. \tag{2.1.7}$$

Where A represents, generalized time dependent co ordinate satisfying the free surface boundary conditions.

The first three modes of liquid in the tank and its frequency were obtained theoretically using the available expressions and compared with the experiments conducted (Table 2.1) . The Fast Fourier Transform of the response signal is shown in Fig. 2.2. which is taken from the bottom pressure guage installed on tank wall.

Calculated sloshing frequency from Eqn. 2.1.6 is 0.78 Hz and experimentally found sloshing frequency is 0.75 Hz and there is very good agreement between experimental and theoretical values. Similar observation was found for the sloshing height also. The photograph showing first mode wave profile is shown in Fig. 2.3. The maximum sloshing height of 61 mm, observed during the experiment was in agreement with the theoretically found value of 58 mm.

2.2. Maximum wave amplitude, dynamic pressures

Sinusoidal harmonic excitation was given at the corresponding sloshing frequency observed. Increased wave amplitudes were observed during the sloshing behaviour. The maximum wave height was found to be 61 mm which is compared with the theoretically available results as per linear theory (Housner, 1963). Table 2.2 give the sloshing height information. During the experiment it was

Table 2.1. Frequency of first three modes from theoretical and experimental investigation

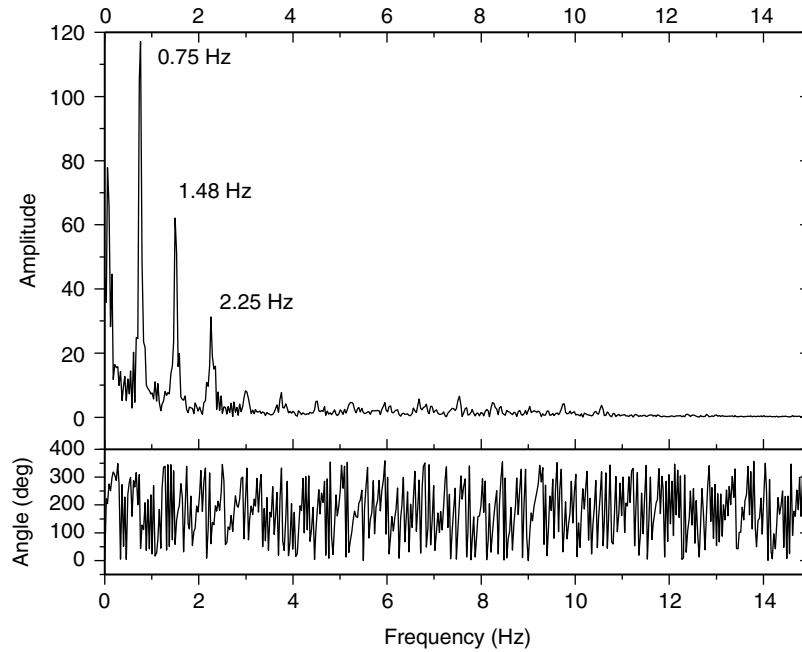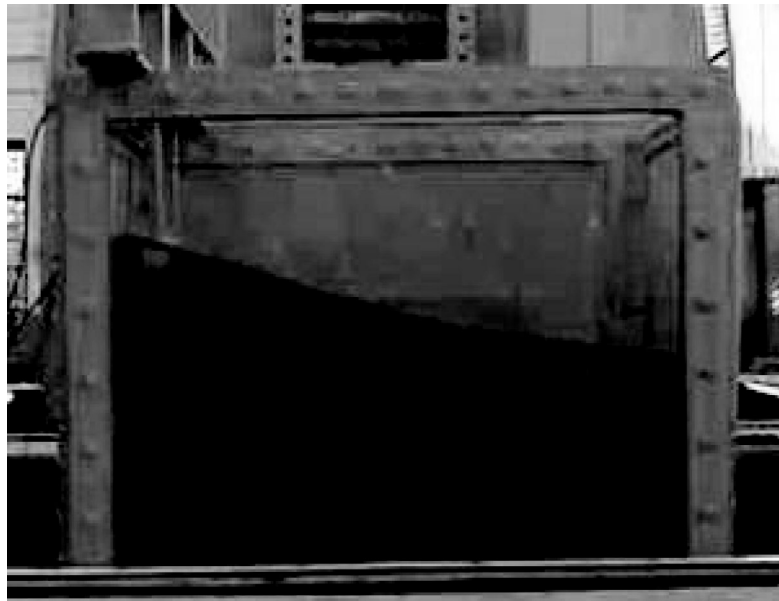| Mode	Frequency (Theoretical), Hz	Frequency (Experimental), Hz
Mode 1 (Anti symmetric)	0.78	0.75
Mode 2 (Anti symmetric)	1.46	1.48
Mode 3 (Anti symmetric)	2.12	2.25

Figure 2.2. Fast Fourier Transform (FFT) of the response signal.

Figure 2.3. First mode observed during the sweep sine experiment.

Table 2.2. Sloshing Wave Height

	Sloshing wave height, mm
Experimental	61
Theoretical	58

observed that the tank wall experienced maximum accelerations corresponding to one of its modal frequencies namely, 12.5 Hz. Free vibration test on the tank and the acrylic wall shows that the natural frequency of wall corresponds to 12.5 Hz which is far away from the sloshing frequency of the liquid.

The sinusoidal sweep tests were conducted with an excellent control of amplitude and acceleration and the measurements were recorded in the forward and reverse sweeps. The pressure time history traces on the wall during the sweep sine test using the three pressure gauges installed are shown in Fig. 2.4. The peak value of the dynamic pressure observed in this case is 3.75 kPa. The maximum pressure registered in sweep sine test is found to be the same as the pressure observed during resonant harmonic testing, as expected. Towards the progressive sweeping with frequencies ranging from 0.5 Hz to 5 Hz, various modal transients and wave breaking phenomena was observed which is of interest. Sweep sine tests gives clear indication of the effect of amplitude and acceleration amplifications and the evolution of nonlinearities in the frequency range 0.25 to 5 Hz. The peak pressure obtained in this case is comparable with the computational steady state (time-periodic) impact pressures with the multimodal method in combination with Wagner theory.
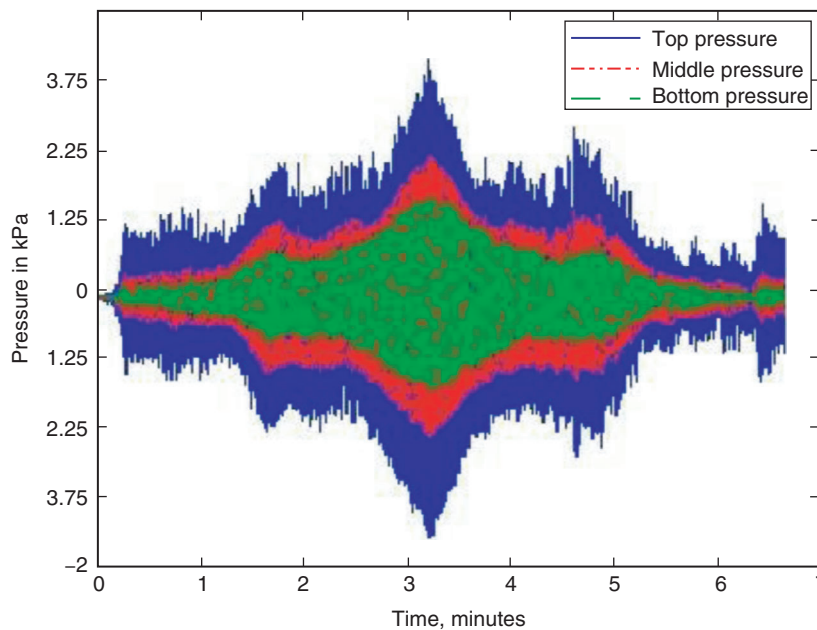

Figure 2.4. Pressures (top, mid and bottom) measured during sweep sine test.

Experiments were continued for harmonic excitation above and below the identified sloshing frequency. During harmonic lateral excitation, different nonlinearities will emerge as large amplitude response or instabilities of various sloshing modes. Very near to the lowest liquid natural frequency rotary sloshing and swirl motion can be observed as witnessed during the experiment. Swirling or rotary wave motions can occur during harmonic horizontal excitation of liquid motion in the nearly square base tanks when the forcing frequency is in the vicinity of the lowest natural frequency. When surface tension is negligible, the maximum downward acceleration exerted on a liquid particle at the free surface, which occurs just when the wave peaks in the upward direction is $g - \delta\omega^2$, where g is the effective gravitational acceleration, δ is the wave amplitude and ω is the slosh natural frequency. As the maximum acceleration at the peak height always remain positive, the maximum wave height cannot be larger than $\delta_{max} = \dfrac{g}{\omega^2}$ and the maximum usually occurs at the tank walls (Faltinsen and Timokha, 2002). As the amplitude of input excitation increases splashing, breaking waves, and even rotary sloshing were observed in the experiment. One such nonlinear behavior is shown in the photograph (Fig. 2.5).

2.3. Investigation on dynamic wave regimes

During harmonic lateral oscillations the steady state response changes from hard spring to soft spring at critical depth. The phase between input displacements and steady state wave elevations is zero, for the frequency ratio $\dfrac{\omega}{\omega_1} < 1$ and is 180^0 when $\dfrac{\omega}{\omega_1} > 1$ in case of planar waves. The phase for swirling
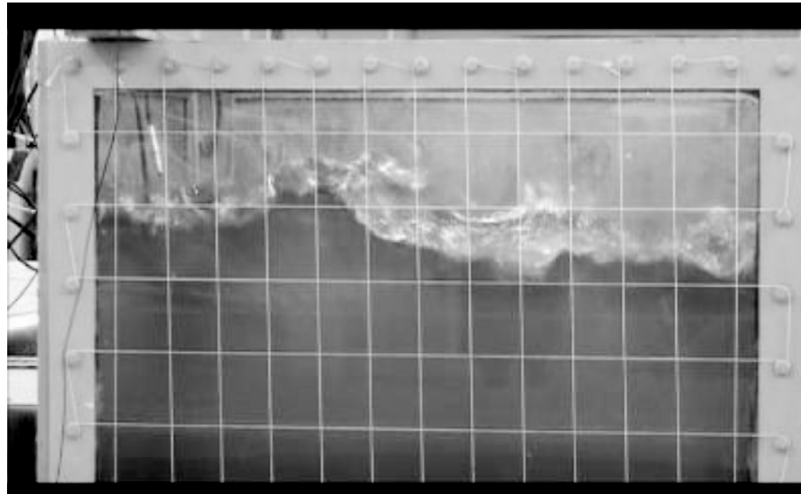
Figure 2.5. The snap shot of nonlinear motion observed during the experiment.

changes from 0 to 180^0. The frequency range of theoretical wave domains has found to be increased for higher forcing amplitudes. The observations are consistent with the results of Royon Lebeaud et al, (2007) who has reported the occurrence of steep waves and strong breaking for swirling with $\dfrac{\omega}{\omega_1} > 1.08$. Here in this case of $h/l = 0.64$, ω/ω_1 is found to be 1.133 that is the largest forcing frequency ratio at which steady state swirling remained stable. The higher response amplification is captured using adaptive modal systems, which accounts for the different kinds of nonlinear energy transfer from primary to higher modes. A small increase in frequency beyond this the swirling suddenly collapses and the wave motion switches to a small amplitude out of phase planar wave. Asymmetric wave profiles were observed during higher amplitude loading and Fig. 2.6. shows the dynamic wave regimes observed during the experiment which was conducted to validate the same for various forcing amplitudes at many frequency ratios. During nonlinear sloshing it is observed that the maximum wave elevations are not the same at the two opposite tank walls. This observation is in tune with the test
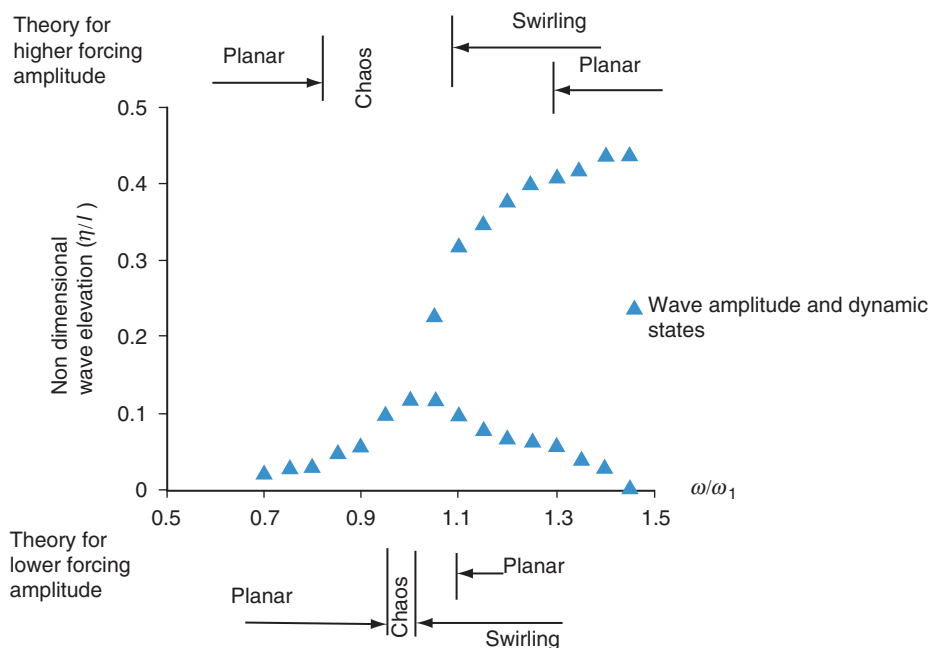

Figure 2.6. Wave amplitude and dynamic states.

results obtained by Colograssi et al (2003). The multimodal method by Faltinsen and Timokha does not recognize this fact. Sub-harmonic oscillations also can be obtained during this regime.

During harmonic lateral excitations various phases of sloshing occurs starting from type 1 to type IV. Type II exhibits steady state oscillations with sub-harmonic behavior. Most of the times during this phase, steady state behavior was interrupted by transient phases. Wave breaking alternate on two sides of the tank. When forcing amplitude is 0.05l it is reported that the time histories of the wave elevations at the two tank walls are quite different and have a clearly nonlinear behavior (Colograssi et al., 2003). During strong nonlinearity free surface fragmentation caused by breaking leads to a shear layer with a higher tangential velocity beneath the free surface which is the cause of the higher maximum run up along the wall other side. The free surface fragmentation is more pronounced during sloshing characterized as type III. The sub-harmonic behavior is more complex than in type II cases with period N times the forcing period, where N is a large number that varies with time. The model tests clearly showed asymmetric behavior of the maximum wave elevation at the two tank sides. In type III, the violent breaking wave phenomena is found to be more concentrated towards one side. The type IV scenario is characterized by the formation of a local splashing jet at a distance from the wall leading to a continuous fragmentation of the free surface. No well defined sub-harmonics exists for this case.

When the wave amplitude is large enough to cause nonlinear effects, the linearized theory is not valid. Neglecting viscous effects, the nonlinear slosh theory can be derived from velocity potential (Eq. 2.1.1) and the liquid velocities are still given by spatial derivatives of the potential. The theory of large amplitude sloshing is described elsewhere (Faltinsen and Timokha, 2002).

The basic differential equation for linear theory is

$$\nabla^2 \Phi = 0. \tag{2.3.1}$$

All the nonlinearities enter the analysis through the boundary conditions. In the linear theory these conditions are imposed at the undisturbed boundaries at the equilibrium locations of the free surface, free surface conditions are imposed. When finite wave amplitudes are considered, however the boundary conditions have to be imposed at the actual locations of the boundaries.

The differences between the linear and nonlinear boundaries for the case of a rectangular tank subjected to a transverse oscillation amplitude X_0 is illustrated in Fig. 2.7. The no flow condition can
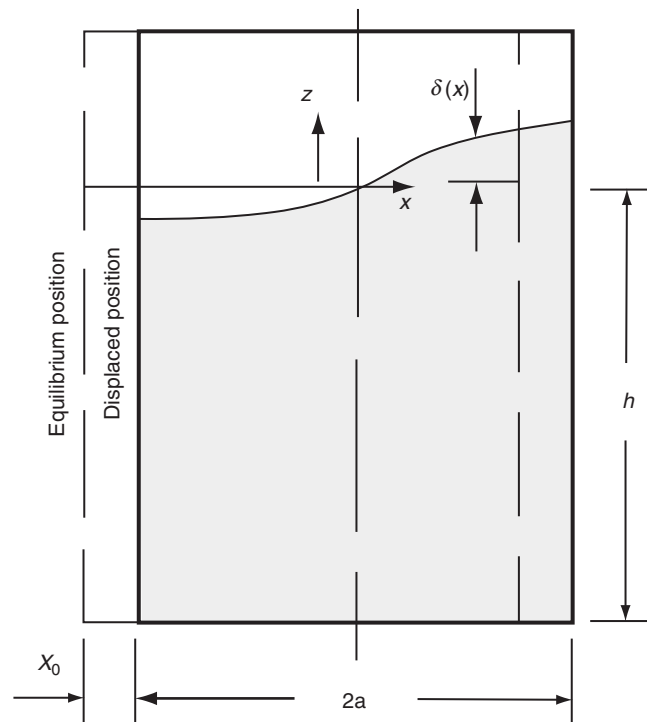

Figure 2.7. Linear and non linear boundaries for a rectangular tank (SP-106, NASA).

be imposed at the displaced condition of the tank walls. The free surface conditions are now imposed on the actual wave surface location, $z = \delta(x, t)$, although this location is unknown and need to be determined as part of the solution.

Assuming the effective gravity is assumed to be acting along the tank axis, and neglecting surface tension effects, and focusing on two dimensional waves in a rectangular tank, u velocities (x-direction) and w velocities (z-direction) need to be considered. The boundary conditions of the tank walls are

$$u = \frac{\partial \Phi}{\partial x} = 0 \text{ for } x = \pm a \tag{2.3.2}$$

$$w = \frac{\partial \Phi}{\partial z} = 0 \text{ for } z = -h \tag{2.3.3}$$

Here for simplicity water depth is assumed to be much greater than the width of the tank. Hence the no flow condition at the tank bottom is replaced by

$$w = \frac{\partial \Phi}{\partial z} = 0 \text{ for } h = -\infty \tag{2.3.4}$$

The nonlinear boundary conditions at the free surface are considerably more complicated than the linear theory boundary conditions. The velocity of the wave perpendicular to the free surface has to be compatible with the liquid velocity at the free surface. Including all the components of liquid velocity as the liquid surface is not flat like earlier and the nonlinear boundary condition becomes:

$$\frac{\partial \delta}{\partial t} = \frac{\partial \Phi}{\partial z} - \frac{\partial \Phi}{\partial x}\frac{\partial \delta}{\partial x} \quad \text{for } z = \delta(x,t) \tag{2.3.5}$$

Similarly, the pressure at the free surface must be made equal to the gas pressure (the value of which can be absorbed into the definition of the potential). The nonlinear boundary condition that relates the pressure and wave motion at the free surface is

$$\frac{\partial \Phi}{\partial t} = -g\delta - \frac{1}{2}\left[\left(\frac{\partial \Phi}{\partial x}\right)^2 + \left(\frac{\partial \Phi}{\partial z}\right)^2\right] \quad \text{for } z = \delta(x,t) \tag{2.3.6}$$

where ϕ denotes the velocity potential and δ the small displacement above the free surface. These equations will be solved by the method of perturbations, which is also called the method of successive approximations (Penney and Price, 1952) which was formulated as part of a World War II effort to compute wave loads on floating breakwaters. Classical Perturbation method (Van Dyke, 1964) applied to nonlinear equations that describe the free surface waves was used to analyze the effects of nonlinearities on sloshing. General purpose computational fluid dynamics computer codes having a free surface capability are usually employed widely to investigate the nonlinear effects. Even though perturbation methods are applicable only over a limited range of wave amplitudes due to convergence considerations, they are still valuable.

2.4. Response to random vibrations

The experiments described in the preceding paragraph could identify the dynamic behaviour of the system and further experiments were continued for a random vibration time history. Fig. 2.8 shows the applied displacement time history on the tri axial table which is in the horizontal direction to the tank. Compared to the harmonic excitation, this represents a larger input amplitude for approximately 40 seconds duration. The applied amplitude of displacement provides a liquid depth
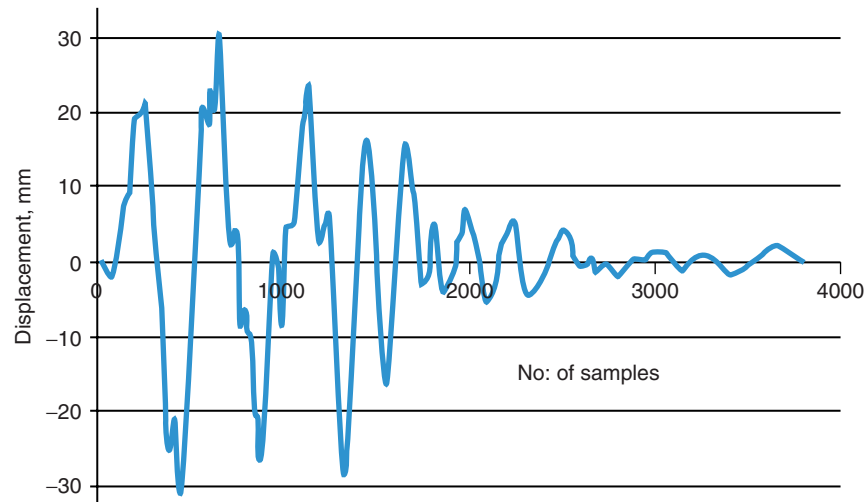
Figure 2.8. Applied random time history to the experimental tank.

to breadth ratio of 0.03. The predominant frequency of the corresponding acceleration spectrum lies in the range 3–4 Hz. A spectrum compatible time history has been generated which contain more energy in the lower frequency domain.

Large amplitude sloshing and significant hydrodynamic pressures were observed on tank walls during the experiment. Fig. 2.9 shows the dynamic pressures observed on the top pressure gauges and it was plotted by the power spectral density via periodogram. The maximum sloshing wave height observed in this case was 160 mm which was almost three times the magnitude recorded at the sloshing frequency of the liquid, namely 0.75 Hz, for which the input forcing amplitude ratio (liquid height to breadth ratio) was 0.0025. As evident from the fig. 2.8, the maximum applied forcing amplitude in this case is 30 mm giving rise to large amplitude sloshing. The maximum pressure obtained in the random excitation is comparable to the maximum pressure observed during the sweep sine tests. The pressure variation on the gauges installed along the height is given in the following figure (Fig. 2.10).
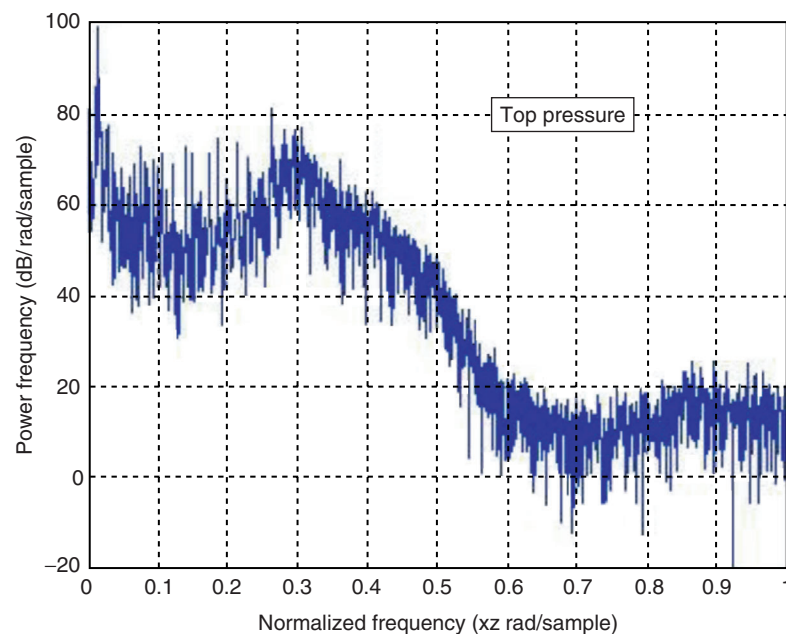

Figure 2.9. Dynamic Pressure-power spectral density via periodogram-observed during the random time history.
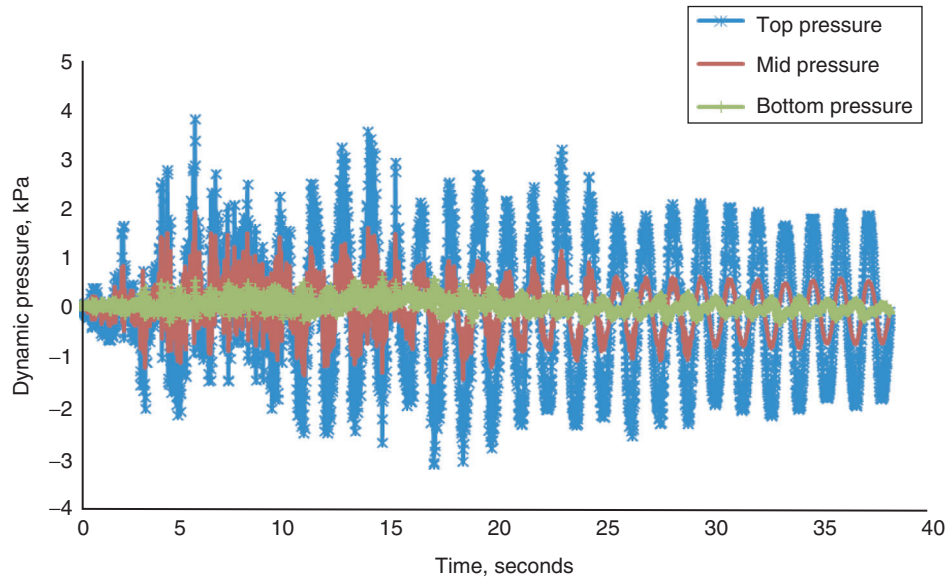
Figure 2.10. The dynamic pressure time history in the top, mid and bottom guages for the applied random displacement record.

As per the linear theory the dynamic pressure evaluated for the tank is 1.8 kPa, at the level of top pressure guage. An increase in peak value of pressure realized during the experiment was of the order of 220 percent (Fig. 2.10). The pressure time variation along the bottom guage is found to be almost same throughout and it is found to be out of phase with the mid and top guage pressure histories. The shape of the hydro-dynamic pressure traces in the mid and top gauges closely resembles the input time histories of acceleration. The top pressure guage shows signs of significant nonlinearity during the initial 20 sec. duration after which it stabilizes as seen in Fig. 2.10.

Free surface elevation recorded during the experiment at the two side walls of the tank for the selected span during the time history (10 to 20 seconds) is shown in Fig. 2.11. Strong nonlinearity is observed during this time as shown in the figure. The inset shows the snapshot of the swirling motion observed during the test. During nonlinear sloshing it is observed that the maximum wave elevations are not the same at the two opposite tank walls. This observation is in tune with the test results obtained by Colograssi et al (2003). Fig. 2.12 shows the difference in corner wave elevations on the two tank walls, which is plotted based on the measured peak values along the length. The measurement was taken at a distance of 0.025 m from the tank wall using the sloshing probe located at the corner.
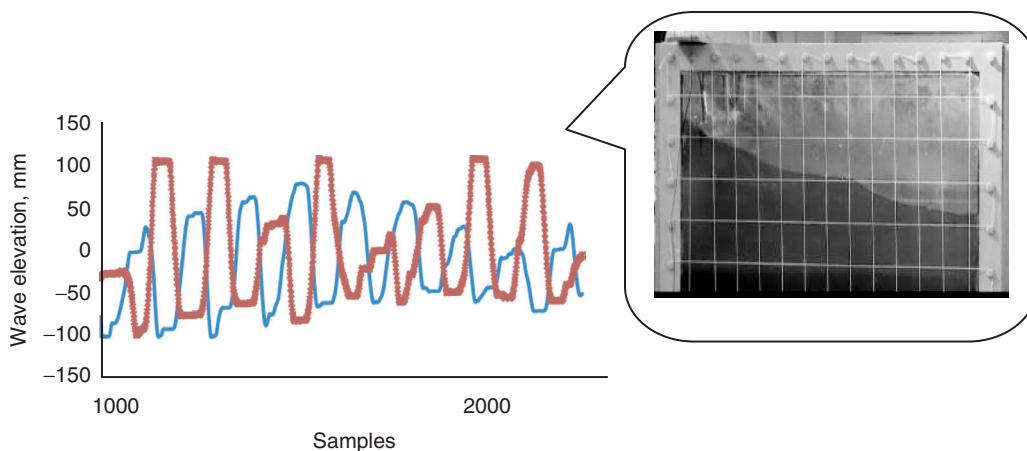

Figure 2.11. Free surface elevation from the experiments at the two side walls of the tank (The observed swirling nonlinearity is shown in insert).
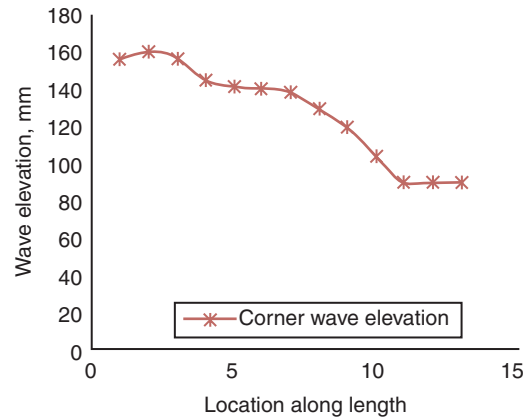
Figure 2.12. Measured wave elevations (corner) along the length of the tank.

3. SALIENT OBSERVATIONS

Traditionally, the small-amplitude wave theory has been used exclusively in evaluating the dynamic performance of liquid-filled containers. As the excitation frequency approaches resonance, the liquid free surface experiences complex motions. It is found from the experiments that the waves follow second order wave theory as evident from the wave profiles. Sinusoidal unidirectional progressive deep water waves are normally represented by first order linear solution which is represented by

$$\zeta = \zeta_a \sin(\omega t - kx) \tag{3.1}$$

where ζ_a denotes wave amplitude, $k = 2\pi/\lambda$, λ being the wave length, $\omega = 2\pi/T$, and it is possible to show that second order velocity potential is zero and the second order wave elevation is ζ_2 which is $\zeta_2 = -1/2\ \zeta_a^2 k \cos[2(\omega t - kx)]$. By combining this with the first-order solution $\zeta_a \sin(\omega t - kx)$, we get

$$\zeta = \zeta_a \sin(\omega t - kx) - 1/2\ \zeta_a^2 k \cos[2(\omega t - kx)] + O((\zeta_a/\lambda)^2) \tag{3.2}$$

Second order theory means that keeping all terms proportional to $O((\zeta_a/\lambda)^2)$ and $O(\zeta_a/\lambda)$ in a consistent way (Faltinsen and Timokha, 2000). Second order wave interaction causes difference frequency effects with energy at the important resonant frequencies, where the first order refers to linear waves. The second order solution given in the Eqn. 3.2 sharpens the wave crests and makes the trough shallower clearly visible during the experiments conducted. The second order wave profile for the wave steepness value, H/λ is found to be 0.049 for the harmonic excitation and reach up to 0.1 in case of severe random excitation. Here H denotes the wave height defined as the vertical distance between the trough and the crest. In all the cases the relative error between second order and infinite order is less than 0.8%. The hydro dynamic pressure observed were found to be higher than the theoretical prediction which is useful for harmonic excitations. It has been observed that top and bottom hydrodynamic pressures are found to be out of phase throughout the tests which can give rise to cross sectional distortions during the strong dynamic inputs.

As the forcing amplitude increases, the nonlinearities become stronger and the pressures on tank walls can be considered equivalent to slamming pressures. For smooth tank, for higher forcing amplitudes, generally surface tension and viscosity do not have a dominant influence on slamming pressures and integrated hydrodynamic loads (Faltinsen and Timokha, 2002). The liquid used for the present experimental investigation is water. It is to be noted that the liquid depth to tank breadth ratio is fixed, an increased tank length increases the highest natural period of liquid flow. Hence higher forcing amplitude excite sloshing around resonance. An equivalent mechanical model of conical pendulum can better describe the non linear effects. Local hydro elastic effects matter when the angle between the impacting free surface and the tank structure is small. A gas cavity can be generated as a consequence of the geometry of the impacting free surface and depending on its size, it may have an important effect of high impact or slamming loads. A Bagnold type model can be used in the presence

of gas cavity. Such impact loads cannot be Froude scaled. When gas cavities influence the impact loads/slamming loads it is emphasized that both Euler and Froude numbers must be the same at model and full scales. A pressure impulse theory can be used to correctly predict the physics. This high slamming pressures are important for the stresses, but its influence on the horizontal force is negligible.

4. COMPUTATIONAL SIMULATION

Regarding modeling the fluid flow, studies related to sloshing and multi modal methods are described elsewhere (Faltinsen and Timokha, 2000). Finite element method for solving the linear floating body hydrodynamic problem is considered by researchers with a hierarchy of boundary damper options for modelling the far field (Krishnankutty and Vendhan, 1995). There are two major problems arising in a computational approach to sloshing. These are the moving boundary conditions at the fluid tank interface and the nonlinear motion of the free surface. Here in the present study interface tracking methods are applied to simulate the fluid behavior within the tank. The study models fluid motion with the incompressible Navier-Stokes formulation (Faltinsen and Timokha, 2000) and the 2D model is used to simulate dynamic free surface flow with the help of a moving mesh. This model describes the fluid dynamics with the incompressible Navier-Stokes equations. There are two types of boundaries in the model domain. Three solid walls, that are modeled with slip conditions, and one free boundary (the top boundary). The harmonic excitation in the tank is modeled using VOF (Volume Of Fraction method) and the sloshing heights are in good agreement. The ALE (Arbitrary Lagrangian-Eulerian) technique has been set up using the moving mesh interface, which represents the free surface boundary with a domain boundary on the moving mesh. Surface tension effects are neglected in the model. The deformation of this mesh relative to the initial shape of the domain is computed using Winslow smoothing. Computational fluid dynamics (CFD) method used can be used for any generally shaped tank with any filling depth and can handle any generic excitation. Even though the model is capable of predicting the sloshing heights it is not efficient to handle the increased pressures and associated nonlinearities like wave breaking accurately for viscous fluids. Here water is used and the the domain equations and boundary conditions used for the simulation are explained in the following paragraph.

4.1. Domain equations

Describing the fluid dynamics with the incompressible Navier-Stokes equations:

$$\rho \frac{\partial \mathbf{u}}{\partial t} + \rho \mathbf{u} \cdot \nabla \mathbf{u} - \nabla \cdot (-p\mathbf{I} + \eta(\nabla \mathbf{u} + (\nabla \mathbf{u})^T)) = \mathbf{F} \qquad (4.1.1)$$

$$\nabla \cdot \mathbf{u} = 0 \qquad (4.1.2)$$

where ρ is the density, $\mathbf{u} = (u, v)$ is the fluid velocity, $\mathbf{p}$ is the pressure, $\mathbf{I}$ is the unit diagonal matrix, η is the viscosity, and $\mathbf{F}$ is the volume force.

    With the help of the Moving Mesh interface, the equations are solved on a freely moving deformed mesh, which constitutes the fluid domain. The deformation of this mesh relative to the initial shape of the domain is computed using Winslow smoothing.

4.2. Boundary conditions for the fluid

The slip boundary condition for the Navier-Stokes equations is

$$\mathbf{u} \cdot \mathbf{n} = 0 \qquad (4.2.1)$$

where $\mathbf{n} = (nx, ny)^T$ is the boundary normal.

    Because the normal vector depends on the degrees of freedom for the moving mesh, a constraint force would act not only on the fluid equations but also on the moving mesh equations. This effect would not be correct, and one remedy is to use weak constraints. Activating the weak constraints to enforce the slip boundary condition without a constraint force acting on the moving mesh equations

$$\hat{\lambda}(\mathbf{u} \cdot \mathbf{n}) - \lambda(\hat{\mathbf{u}} \cdot \mathbf{n}) \qquad (4.2.2)$$

for some Lagrange multiplier variable λ. Here λ and $\check{U}$ denote test functions.

The fluid is free to move on the top boundary. The stress in the surrounding environment is neglected.

Therefore the stress continuity condition on the free boundary is

$$(-\mathbf{pI} + \eta(\nabla\mathbf{u} + (\nabla\mathbf{u})^\mathbf{T}))\cdot \boldsymbol{n} = -\mathbf{p_0}\mathbf{n} \tag{4.2.3}$$

where p_0 is the surrounding (constant) pressure and η the viscosity of the fluid. Without loss of generality, $p_0 = 0$ for this model.

4.3. Boundary conditions for the mesh

In order to follow the motion of the fluid with the moving mesh, the mesh motion to the fluid motion normal to the surface is coupled. It is not desirable to couple in the tangential direction as the mesh soon becomes so deformed that the solution no longer converges. The boundary condition for the mesh equations on the free surface is therefore

$$(x_t y_t)^T \cdot \mathbf{n} = \mathbf{u}\cdot\mathbf{n} \tag{4.3.1}$$

where n is the boundary normal and $(x_t, y_t)^T$ the velocity of mesh.

In the Moving Mesh interface, we specify this boundary condition by selecting the tangent and normal coordinate system in the deformed mesh and by specifying a mesh velocity in the normal direction, where you enter the right-hand side expression from above as $u*n_x+v*n_y$. For this boundary condition with the weak constraints activated, Moving Mesh interface adds the weak expression

$$\hat{\lambda}(((x_t y_t)^T - \mathbf{u})\cdot\mathbf{n}) - \lambda((\hat{x}\hat{y})^T \cdot \mathbf{n}) \tag{4.3.2}$$

to ensure that there are no constraint forces acting on the fluid equations. Here again, λ denotes some Lagrange multiplier variable (not the same as before) and, $\check{\lambda}$, $\hat{x}$ and $\hat{y}$ denote test functions.

Later on level set methods for the two phases have been implemented which represent the interface by a contour of a smooth function with good mass conservation while considering the three dimensional free surface flows. A phase field method has been implemented for the two phase laminar flow. The simulated model can well determine the sloshing wave heights and the dynamic behavior including pressures, during the harmonic excitation. The simulation results are shown at various timings. Fig. 3.1 and Fig. 3.2 shows the experimentally observed behavior and the computational modeling of sloshing.
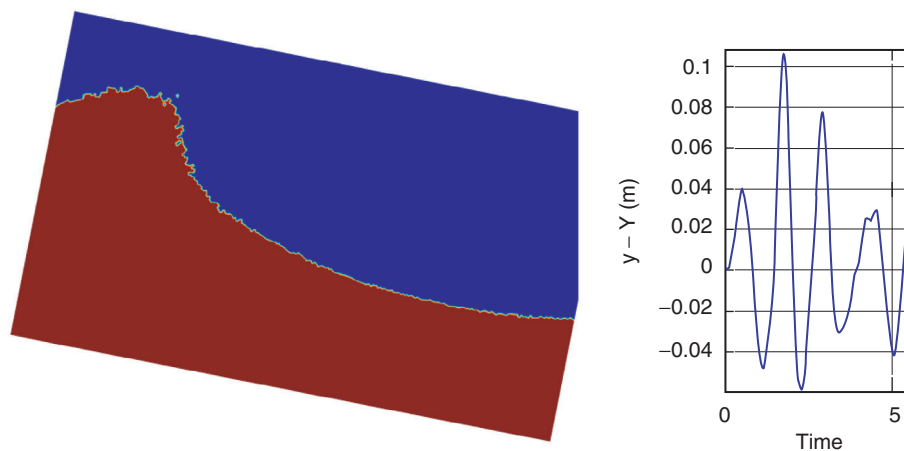
Figure 3.1. Computational simulation of Sloshing –Typical snapshot and the observed sloshing height in m for 5 seconds.
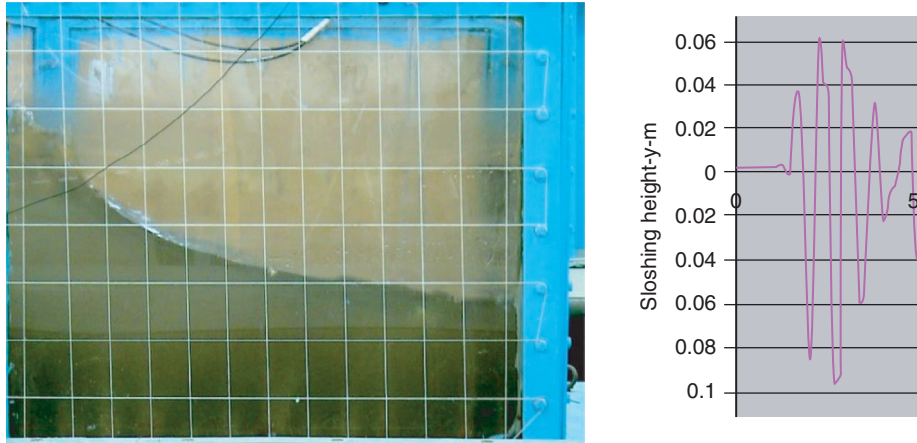
Figure 3.2. Experimentally observed Sloshing –Typical snapshot and the experimentally observed sloshing height in mm for 5 seconds.

5. CONCLUSIONS

The tests reported herein have demonstrated the dynamic sloshing behavior of water in nearly square based anchored tanks experimentally in three dimensions. The study is motivated by the discrepancy observed between previous quantitative theoretical results and experimental measurements in two dimensions. The observed hydro dynamic pressures and the difference in wave elevations are significant for the design of this class of structures. Large amplitude sloshing was simulated in a tri-axial shaking table and the nonlinear sloshing behavior was investigated. The non-linear sloshing effects are manifested by the amount of upward shifting of the wave during sloshing and the hydro dynamic pressure on tank walls. The maximum hydro dynamic pressure is observed towards the top surface and is found to increase nonlinearly in case of large amplitude forced vibration. It has been observed that top and bottom hydrodynamic pressures are found to be out of phase throughout the tests which can give rise to cross sectional distortions during strong dynamic events. Normally tank walls are designed for the beam like responses predicted by the analysis procedures and the cross sectional distortions as evident from many of the base excitations have been attributed to the imperfections in the geometry or fabrication. The experiments conducted throws light into the physics related the dynamic phenomena. Large amplitude sloshing with higher rate of loading can impart significant dynamic peak fluid pressure on tank walls and the localized stress amplification need to be accounted in the design of liquid storage tanks.

ACKNOWLEDGEMENT

REFERENCES

Abramson, H. N. (1966). The dynamic behaviour of liquids in moving containers', NASA SP-106, National Aeronautics and Space Administration, Washington DC.

Abramson HN, Bass RL, Faltinsen O, and Olsen HA (1974), Liquid Slosh in LNG Carriers, 10th Symp Naval Hydrodynamics, MIT, Cambridge, MA.

American Water Works Association (AWWA). AWWA Standards for Welded Steel Tanks for Water Storage. *ANSI/AWWA* 1996; 100-96.

API 650 – 11th Edition, Welded Steel Tanks for Oil Storage. *American Petroleum Institute, Washington*, D.C., USA 2007.

Bagnold, R A., (1939) Interim report on wave pressure research. Journal of the Institution of Civil Engineers, London 12, 202–225.

Colagrossi A, Lugni C, Dousset V, Bertram V, and Faltinsen O M (2003). Numerical and experimental study of sloshing in partially filled rectangular tanks. Proceedings of the 6th numerical towing tank symposium, Rome.

Colagrossi A (2005). A meshless lagrangean method for free surface and interface flow, Ph-D Thesis, University of Rome, La Sapienza.

Faltinsen, O.M., Rognebakke, O. F., Lukovsky, I.A. and Timokha A N. (2000) Multidimensional modal analysis of nonlinear sloshing in a rectangular tank with finite water depth. *Journal of Fluid Mechanics* **407**, 201–234.

Faltinesn O. M. and Timokha A. N. (2002), Asymptotic modal approximation of nonlinear resonant sloshing in a rectangular tank with small fluid depth, *Journal of Fluid Mechanics*. **470**, 319–357.

Graham EW and Rodriguez AM (1952), The characteristics of fuel motion which affect airplane dynamics, J Appl Mech 74, 381–388.

Hatayama, K. (2008). Lessons from the 2003 Tokachi-oki, Japan, earthquake for prediction of long-period strong ground motions and sloshing damage to oil storage tanks. *Journal of Seismology* **12**, 255–263.

Henderson D.M and Miles J. W (1994), Surface-wave damping in a circular cylinder with a fixed contact-line, J Fluid Mech 275, 285–299.

Hill D.F., Transient and steady-state amplitudes of forced waves in rectangular basins, Phys. Fluids 15 (2003) 1576–1587.

Housner GW(1963). The Dynamic Behavior of Water Tanks. *Bulletin of Seismological Society of America*. **53(2)**, 381–387.

Ibrahim, R. A., Liquid Sloshing Dynamics, Theory and Applications. Cambridge University Press, 2005.

Kana DD (1966), An Experimental Study of Liquid Surface Oscillations in Longitudinally Excited Compartmented Cylindrical and Spherical Tanks, NASA CR-545.

Kim Y. (2001), Numerical simulation of sloshing flows with impact load, Appl. Ocean Res. 23 (1), 53–62.

Kim Y., Park Y. J., and Lee H. R. (1994), A numerical study on the prediction of sloshing impact pressure, Trans. Soc. Naval Arch. Korea 30(4), 61–73.

Krishnankutty, P. and Vendhan, C.P. (1995). Three-dimensional finite element analysis of the diffraction-radiation problem of hydrodynamically compact structures, *Marine Structures* **8:5**, 525–542.

Manos, G.C. and Clough, R.W. (1985). Tank damage during the may 1983 Coalinga earthquake. *Earthquake Engineering and Structural Dynamics* **13**, 449–466.

Miles JW (1991), Wave motion in a viscous fluid of variable depth: moving contact-line, J Fluid Mech 223, 47–55.

Moiseyev, N. N., 1958, On the Theory of Nonlinear Vibrations of a Liquid of Finite Volume, Appl. Math. Mech., 22, pp. 860–870.

Penney WG and Price AT (1952), Finite periodic stationary waves in a perfect liquid - Part II, Phil Trans Royal Soc (London) 254–284.

Royon-Lebeaud, A., Hopfinger E.J., and Cartellier, A. (2007) Liquid Sloshing and Wave breaking in circular and square – base cylindrical containers. *Journal of Fluid Mehanics* **577**, 467–494.

Rafiee A. Pistani F and Thiagarajan K. (2011) Study of liquid sloshing: numerical and experimental approach. *Computational Mechanics :* **47**: 65–75.

Scarsi G (1971), Natural frequencies of viscous liquids in rectangular tanks, Meccanica 6(4), 223–234.

Sengupta T K, Guntaka A, and Dey S (2004), Solving Navier Stokes equation for flow past cylinders using single – block structured and over set grids, *Journal of Scientific Computing*, 21(3), 269–282: DOI: 10.1007/s10915-004-1318-1.

Sengupta T K, Suman V K, and Neelu Singh (2010), Solving Navier Stokes equation for flow past cylinders using single – block structured and over set grids, *Journal of Computational Physics*, 229(1), 178–199.

Sreekala, R., Muthumani, K., Prasad, A. M. and Nagesh, R, Iyer. (2011). Pulse like ground motions-Quantification on damage severity. *SmiRT-21*, Book of Abstracts **Vol. 1**, 459.

Su T. C. (1981), The effect of viscosity on free oscillations of fluid-filled spherical shells, J. Sound. Vib. 74(2), 205–220.

Tadasi Watanabe (2011) Numerical simulation of liquid sloshing using Arbitrary Langrangean Eulerian Level set method, *The International Journal of Multiphysics*, **5(4)**, 339–352.

Van Dyke, M., 1998, Identification of Influential Factors for Liquid Acquisition Device Designs, AIAA Paper 98-3198.

Wagner C, Miiller HW, and Knorr K (1999), Faraday waves on a viscoelas-tic liquid, Phys Rev Lett 83, 308–311.